

# Constraining the cosmological parameters with the gas mass fraction in local and $z > 0.7$ Galaxy Clusters

S. Ettori<sup>1</sup>, P. Tozzi<sup>2</sup>, and P. Rosati<sup>1</sup>

<sup>1</sup> ESO, Karl-Schwarzschild-Str. 2, D-85748 Garching, Germany

<sup>2</sup> INAF, Osservatorio Astronomico di Trieste, via Tiepolo 11, I-34131 Trieste, Italy

Accepted on 14th Nov 2002

**Abstract.** We present a study of the baryonic fraction in galaxy clusters aimed at constraining the cosmological parameters  $\Omega_m$ ,  $\Omega_\Lambda$  and the ratio between the pressure and density of the “dark” energy,  $w$ . We use results on the gravitating mass profiles of a sample of nearby galaxy clusters observed with the *BeppoSAX* X-ray satellite (Ettori, De Grandi & Molendi, 2002) to set constraints on the dynamical estimate of  $\Omega_m$ . We then analyze *Chandra* observations of a sample of eight distant clusters with redshift in the range 0.72 and 1.27 and evaluate the geometrical limits on the cosmological parameters  $\Omega_m$ ,  $\Omega_\Lambda$  and  $w$  by requiring that the gas fraction remains constant with respect to the look-back time. By combining these two independent probability distributions and using *a priori* distributions on both  $\Omega_b$  and  $H_0$  peaked around primordial nucleosynthesis and HST-Key Project results respectively, we obtain that, at 95.4 per cent level of confidence, (i)  $w < -0.54$ , (ii)  $\Omega_m = 0.34^{+0.11}_{-0.05}$ ,  $\Omega_\Lambda = 1.50^{+0.24}_{-1.13}$  for  $w = -1$  (corresponding to the case for a cosmological constant), and (iii)  $\Omega_m = 1 - \Omega_\Lambda = 0.33^{+0.06}_{-0.05}$  for a flat Universe. These results are in excellent agreement with the cosmic concordance scenario which combines constraints from the power spectrum of the Cosmic Microwave Background, the galaxy and cluster distribution, the evolution of the X-ray properties of galaxy clusters and the magnitude-redshift relation for distant type Ia supernovae. By combining our results with the latter method we further constrain  $\Omega_\Lambda = 0.94^{+0.30}_{-0.30}$  and  $w < -0.89$  at the  $2\sigma$  level.

**Key words.** galaxies: cluster: general – galaxies: fundamental parameters – intergalactic medium – X-ray: galaxies – cosmology: observations – dark matter.

## 1. INTRODUCTION

Several tests have been suggested to constrain the geometry and the relative amounts of the matter and energy constituents of the Universe (see recent review in Peebles & Ratra 2002 and references therein). A method that is robust and complementary to the others is obtained using the gas mass fraction,  $f_{\text{gas}} = M_{\text{gas}}/M_{\text{tot}}$ , as inferred from X-ray observations of clusters of galaxies. In this work, we consider two independent methods for our purpose: (i) we compare the relative amount of baryons with respect to the total mass observed in galaxy clusters to the cosmic baryon fraction to provide a direct constraint on  $\Omega_m$  (this method was originally adopted to show the crisis of the standard cold dark matter scenario in an Einstein-de Sitter Universe from White et al. 1993), (ii) we limit the parameters that describe the geometry of the universe assuming that the gas fraction is constant in time, as firstly suggested by Sasaki (1996).

The outline of our work is the following. In Section 2, we describe the cosmological framework that allows us to formulate the cosmological dependence of the cluster gas mass frac-

tion. In Section 3, we use a sample of nearby clusters to constrain mainly the cosmic matter density. Eight galaxy clusters with  $z > 0.7$  are then presented and analyzed in Section 4 and a further constraint on the geometry of the Universe is given under the assumption of a constant gas fraction as function of redshift. A description of the systematic uncertainties that affect our estimates is discussed in Section 5. Finally, the combined probability function and the overall cosmological constraints (also considered in combination with results from SN type Ia magnitude-redshift diagram) are described in Section 6 along with prospective for future work.

## 2. THE COSMOLOGICAL FRAMEWORK

We refer to  $\Omega_m$  as the *total* matter density (i.e., the sum of the *cold* and *baryonic* component:  $\Omega_m = \Omega_c + \Omega_b$ ) in unity of the critical density,  $\rho_c = 3H_0^2/(8\pi G)$ , where  $H_0 = 100h \text{ km s}^{-1} \text{ Mpc}^{-1}$  is the Hubble constant and  $G$  is the gravitational constant, and to  $\Omega_\Lambda$  as the constant energy density associated with the “vacuum” (Carroll et al. 1992). We consider a generalization from this static, homogeneous energy component to a dynamical, spatially inhomogeneous form of energy with still a negative pressure, or “quintessence” (e.g. Turner & White 1997, Caldwell et al. 1998). We neglect the energy asso-

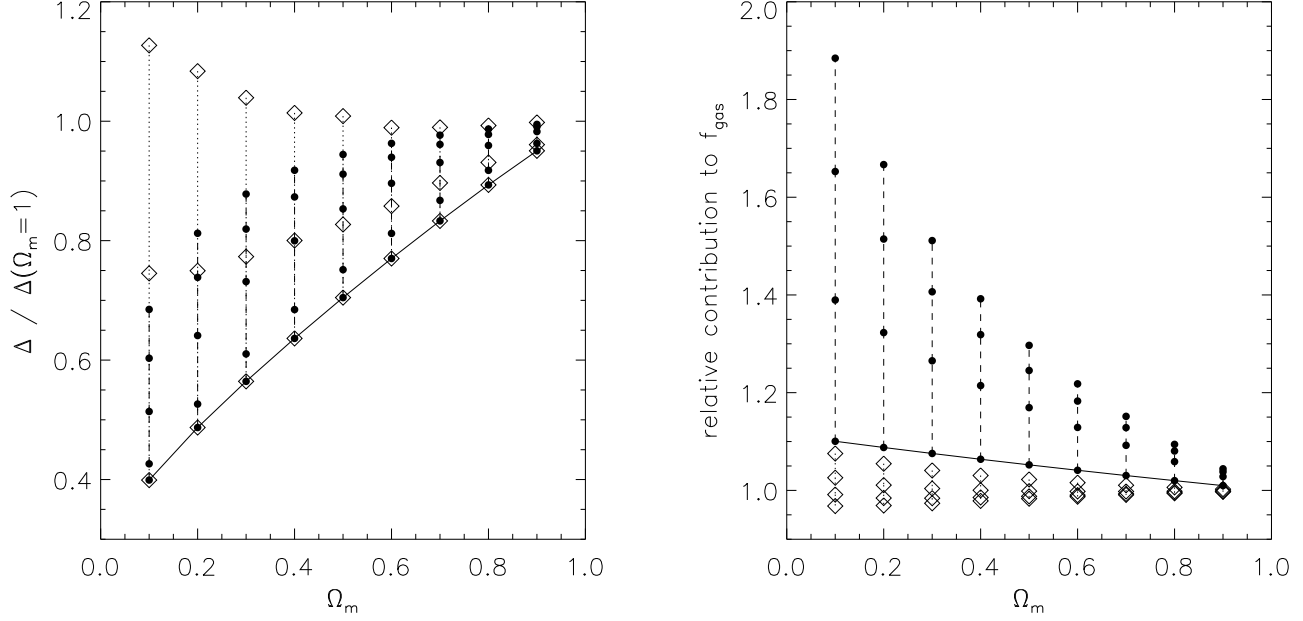


**Fig. 1.** (Left) Values of the density contrast  $\Delta$  (with respect to what expected for an Einstein -de Sitter model) of the density contrast  $\Delta$  estimated in an “ $\Omega_m + \Omega_\Lambda = 1$ ” universe at redshift 0, 0.1, 0.4, 0.7 and 1 (filled circles, from bottom to top, respectively) and with  $w$  equal to  $-0.2, -0.6, -1$  (diamonds, from top to bottom, respectively; solid line: values at  $z = 0$  for  $w = -1$ ). (Right) Plot of the multiplicative factors that correct the gas fraction with respect to the initial estimate computed within a density contrast of 1500 in an Einstein -de Sitter universe: corrections due to the dependence upon  $d_{\text{ang}}^{3/2}$  (filled circles, at  $z = 0.1, 0.4, 0.7$  and 1, starting from the bottom, respectively) and the change due to the density contrast (diamonds; solid line: values at  $z = 0.1$ ).

ciated to the radiation of the cosmic microwave background,  $\Omega_r \approx 5 \times 10^{-5}$ , and any possible contributions from light neutrinos,  $\Omega_\nu = (\sum \mu_\nu / h^2) / 92.5 \text{ eV}$ , that is expected to be less than 0.05 for a total mass in neutrinos,  $\sum \mu_\nu$ , lower than 2.5 eV (see, e.g., the recent constraints from 2dF galaxy survey in Elgaroy et al. 2002 and from combined analysis of cosmological datasets in Hannestad 2002). Thus, we can write  $\Omega_m + \Omega_\Lambda + \Omega_k = 1$ , where  $\Omega_k$  accounts for the curvature of space.

In this cosmological scenario, the angular diameter distance can be written as (e.g. Carroll, Press & Turner 1992, cf. eqn. 25)

$$d_{\text{ang}} = \frac{c}{H_0(1+z)} \frac{S(\omega)}{|\Omega_k|^{1/2}}, \quad \omega = |\Omega_k|^{1/2} \int_0^z \frac{d\zeta}{E(\zeta)}, \quad (1)$$

where  $S(\omega)$  is  $\sinh(\omega)$ ,  $\omega, \sin(\omega)$  for  $\Omega_k$  greater than, equal to and less than 0, respectively, and

$$E(z) = [\Omega_m(1+z)^3 + \Omega_k(1+z)^2 + \Omega_\Lambda(1+z)^{3+3w}]^{1/2} \quad (2)$$

that includes the dependence upon the ratio  $w$  between the pressure and the energy density in the equation of state of the dark energy component (Caldwell, Dave & Steinhardt 1998, Wang & Steinhardt 1998). Hereafter we consider a pressure-to-density ratio  $w$  constant in time (see, e.g., Huterer & Turner 2001, Gerke & Efstathiou 2002 for the extension of eqn. 2 to a redshift-dependent form). In particular, the case for a cosmological constant  $\Lambda$  requires  $w = -1$ .

## 2.1. The cosmological dependence of the observed Cluster Gas Mass Fraction

We assume that galaxy clusters are spherically symmetric gravitationally bound systems. For each galaxy cluster observed at redshift  $z$ , we evaluate the gas mass fraction at  $r_\Delta$ ,  $f_{\text{gas}}(r_\Delta) = M_{\text{gas}}(< r_\Delta) / M_{\text{tot}}(< r_\Delta)$ , where  $r_\Delta$  is defined according to the dark matter profile,  $M_{\text{tot}}(< r)$ , for a fixed density contrast  $\Delta = M_{\text{tot}}(< r_\Delta) / (4\pi \rho_{c,z} r_\Delta^3)$ . In the latter equation,  $\rho_{c,z}$  is the critical density at redshift  $z$  and is equal to  $3H_z^2 / (8\pi G)$  with  $H_z = H_0 E(z)$  (see eqn. 2). In the following sections, we describe how the dark matter mass profile is obtained for each object and which density contrast we adopt initially in an Einstein-de Sitter universe.

The assumed cosmological model affects the definition of the gas mass fraction,  $f_{\text{gas}}(r_\Delta)$ , given above in two independent ways:

1. for a galaxy cluster observed at redshift  $z$  up to a characteristic angular radius  $\theta_c$  and with an X-ray flux  $S_X = L_X(1+z)^{-4} / (4\pi d_{\text{ang}}^2) \propto M_{\text{gas}}^2 \theta_c^{-3} d_{\text{ang}}^{-3} / d_{\text{ang}}^2$  [where the X-ray luminosity  $L_X \approx n_{\text{gas}}^2 \Lambda(T_{\text{gas}}) \times \theta_c^3 d_{\text{ang}}^3$ , and  $\Lambda(T_{\text{gas}})$  is the cooling function of the X-ray emitting plasma that depends only on the plasma temperature] and a total mass,  $M_{\text{tot}}$ , estimated through the equation of the

hydrostatic equilibrium, the measured gas mass fraction is

$$f_{\text{gas}} = \frac{M_{\text{gas}}}{M_{\text{tot}}} \propto \frac{S_X^{1/2} \theta_c^{3/2} d_{\text{ang}}^{5/2}}{\theta_c d_{\text{ang}}} \propto d_{\text{ang}}(z, \Omega_m, \Omega_\Lambda, w)^{3/2}, \quad (3)$$

2. the density contrast,  $\Delta$ , depends upon the redshift and the cosmological parameters.

We have initially evaluated the gas fraction,  $f_{\text{gas}}(\Delta_{\Omega_m=1})$ , in an Einstein-de Sitter universe with a Hubble constant of 50 km s<sup>-1</sup> Mpc<sup>-1</sup>. Then, we change the set of cosmological parameters and evaluate for each cluster at redshift  $z$  the new values of the angular diameter distance  $d_{\text{ang}}$  and the density contrast with respect to the critical density at that redshift. This density contrast is calculated according to the formula in Lokas & Hoffman (2001, Sect. 4.2) for a “ $\Omega_m + \Omega_\Lambda + \Omega_k = 1$ ” universe and in Wang & Steinhardt (1998, eqn. 5, 7 and A11; note that these formulae are estimated for a background density that is  $\Omega_m(z)$  times the critical density) for a “quintessence” flat model (see left panel in Fig. 1).

Since we want to consider the gas fraction in each cluster estimated within the same  $\Delta$  for any given set of cosmological parameters, we therefore multiply  $f_{\text{gas}}(\Delta_{\Omega_m=1})$  by two factors, the first one that rescales the distance,  $F_1 = (d_{\text{ang}, \Omega_m, \Omega_\Lambda, w} / d_{\text{ang}, \Omega_m=1})^{3/2}$ , and the second one that corrects by the change in the density contrast,  $F_2 = (\Delta_{\Omega_m, \Omega_\Lambda, w} / \Delta_{\Omega_m=1}) \times (H_z^2 d_{\text{ang}}^2)_{\Omega_m=1} / (H_z^2 d_{\text{ang}}^2)_{\Omega_m, \Omega_\Lambda, w}$ , where in the latter factor  $M_{\text{tot}}(< r_\Delta)$  and the angular radius  $\theta_\Delta = r_\Delta / d_{\text{ang}}$  are given (see right panel in Fig. 1). In particular, being  $\Delta \propto r_\Delta^{-2}$  and  $f_{\text{gas}} \propto r_\Delta^{0.2}$  (e.g. Ettori & Fabian 1999a, and figure 13 in Frenk et al. 1999), we conclude that

$$f_{\text{gas}, \Omega_m, \Omega_\Lambda, w} = f_{\text{gas}, \Omega_m=1} \times F_1 \times F_2^{-0.1}. \quad (4)$$

As shown in Fig. 1, the second correction affects the  $f_{\text{gas}}$  values by less than 10 per cent and is marginal with respect to the cosmological effects due to the dependence upon the angular diameter distance. We apply both these corrections to evaluate each cluster gas fraction in the following analysis.

### 3. FIRST CONSTRAINT: $\Omega_m$ FROM THE GAS FRACTION VALUE

In this section, we describe how the local estimate of gas mass fraction provides a robust constraint on the cosmic matter density. We make use of the further assumption of a constant gas fraction with redshift in the next section, where we consider a sample of galaxy clusters with  $z > 0.7$ .

The observational constraints on the abundance of the light elements (e.g. D, <sup>3</sup>He, <sup>4</sup>He, <sup>7</sup>Li) in the scenario of the primordial nucleosynthesis gives a direct measurement of the baryon density with respect to the critical value,  $\Omega_b$ . Moreover, the BOOMERANG, MAXIMA-1 and DASI experiments have recently shown that the second peak in the angular power spectrum of the cosmic microwave background provides a constraint on  $\Omega_b$  completely consistent with the one obtained from calculations on the primordial nucleosynthesis (e.g. de Bernardis et al. 2002).

**Table 1.** The local sample from *BeppoSAX* MECS observations. The quoted values are obtained from the deprojection of the spectral results and assuming a functional form of the total mass profile (see Ettori et al. 2002 for details). A Hubble constant of 50 km s<sup>-1</sup> Mpc<sup>-1</sup> is considered in an Einstein-de Sitter universe.

cluster	$z$	$T_{\text{mw}}(r_\Delta)$	$f_{\text{gas}}(r_\Delta)$
$\Delta = 1500$			
A85	0.0518	$5.77 \pm 0.32$	$0.121 \pm 0.008$
A426	0.0183	$7.31 \pm 0.16$	$0.172 \pm 0.009$
A1795	0.0632	$5.53 \pm 0.27$	$0.130 \pm 0.009$
A2029	0.0767	$7.68 \pm 0.46$	$0.126 \pm 0.007$
A2142	0.0899	$8.47 \pm 0.46$	$0.176 \pm 0.011$
A2199	0.0309	$4.53 \pm 0.21$	$0.123 \pm 0.009$
A3562	0.0483	$4.82 \pm 0.64$	$0.117 \pm 0.027$
A3571	0.0391	$5.91 \pm 0.33$	$0.104 \pm 0.009$
PKS0745	0.1028	$8.36 \pm 0.47$	$0.143 \pm 0.009$
$\Delta = 500$			
A85	0.0518	$4.84 \pm 0.27$	$0.134 \pm 0.011$
A426	0.0183	$8.12 \pm 0.17$	$0.235 \pm 0.015$
A1795	0.0632	$4.59 \pm 0.22$	$0.122 \pm 0.013$
A2029	0.0767	$6.30 \pm 0.37$	$0.142 \pm 0.011$
A2142	0.0899	$7.19 \pm 0.34$	$0.203 \pm 0.018$
A2199	0.0309	$4.21 \pm 0.20$	$0.183 \pm 0.014$
A3571	0.0391	$4.24 \pm 0.23$	$0.132 \pm 0.017$
PKS0745	0.1028	$8.81 \pm 0.50$	$0.126 \pm 0.012$

If the regions that collapse to form rich clusters maintain the same ratio  $\Omega_b / \Omega_c$  as the rest of the Universe, a measurement of the cluster baryon fraction and an estimate of  $\Omega_b$  can then be used to constrain the “cold”, and more relaxed, component of the total matter density. This method alone can not provide a reliable limit on the amount of the mass-energy presents in the Universe as *hot* constituents (e.g. WIMPS, like massive neutrino) or energy of the field (e.g.  $\Omega_\Lambda$ , quintessence), as both do not cluster on scales below 50 Mpc.

X-ray observations show that the dominant component of the luminous baryons is the X-ray emitting gas that falls into the cluster dark matter halo. Therefore, the gas fraction alone provides a reasonable upper limit on  $\Omega_c$ :

$$\Omega_c < \frac{\Omega_b}{f_{\text{gas}}} \propto h^{-1/2}, \quad (5)$$

where the dependence of the ratio  $\Omega_b / f_{\text{gas}}$  on the Hubble constant is factored out (White et al. 1993, White & Fabian 1995, David, Jones & Forman 1995, Evrard 1997, Ettori & Fabian 1999a, Mohr, Mathiesen & Evrard 1999, Roussel, Sadat & Blanchard 2000, Erdogdu, Ettori & Lahav 2002, Allen, Schmidt & Fabian 2002).

To assess this limit, we use the gas mass fraction estimated in nearby massive galaxy clusters selected to be relaxed, cooling-flow systems with mass-weighted  $T_{\text{gas}} > 4$  keV from the sample presented in Ettori, De Grandi & Molendi (2002; cf. Table 1). To date, this sample is the largest for which the physical quantities (i.e. profiles of gas density, temperature, luminosity, total mass, etc.) have all been derived simultaneously from spatially-resolved spectroscopy of the same dataset

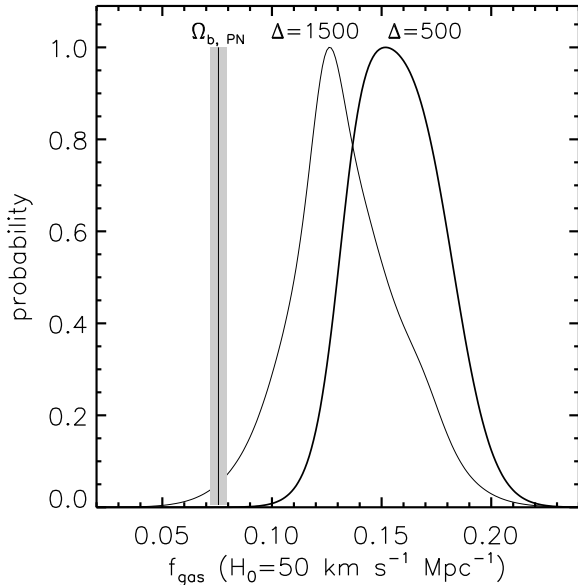


**Fig. 2.** Probability distributions (see Press 1996) at different density contrast  $\Delta$  of the values of the gas mass fraction for cooling-flow clusters with  $T_{\text{gas}} > 4$  keV from the sample in Ettori, De Grandi & Molendi (2002). The central and  $1 - \sigma$  values are  $(0.126, 0.024)$  and  $(0.152, 0.020)$  at  $\Delta = 1500$  and  $500$ , respectively. These values have to be compared with the mean and standard deviation of  $(0.134, 0.025)$  and  $(0.152, 0.043)$ , respectively. The estimated  $\Omega_b$  from primordial nucleosynthesis results (Burles et al. 2001) is overplotted for comparison.

(*BeppoSAX* observations, in this case). Through the deprojection of the spectral results, and assuming a functional form for the dark matter distribution to be either a King (King 1962) or a Navarro, Frenk & White (1997) profile, the gas and total mass profiles are recovered in a self-consistent way. Hence, the density contrast,  $\Delta = M_{\text{tot}}(< r_\Delta) / (4\pi\rho_{c,z}r_\Delta^3)$ , and the gas fraction at  $r_\Delta$ ,  $f_{\text{gas}}(r_\Delta) = M_{\text{gas}}(< r_\Delta) / M_{\text{tot}}(< r_\Delta)$ , can be properly evaluated.

In Fig. 2, we compare the estimated  $\Omega_b$  from primordial nucleosynthesis calculation with the probability distribution (obtained following a Bayesian approach discussed in Press 1996) of the values of the gas mass fraction for nine (at  $\Delta = 1500$ ) and eight (at  $\Delta = 500$ ) nearby massive objects. This plot shows that at lower density contrast (i.e. larger radius) the amount of gas mass tends to increase relatively to the underlying dark matter distribution. Even if there is indication that the gas fraction becomes larger moving outward and within the virialized region, we decide to adopt  $f_{\text{gas}}$  at  $\Delta = 500$  as representative of the cluster gas fraction. In fact, at  $\Delta = 500$  the gas fraction is expected to be not more than 10 per cent less than the universal value, a difference which is smaller than our statistical error, and in any case is likely to be swamped by other effects (see comments in the first item in Section 5).

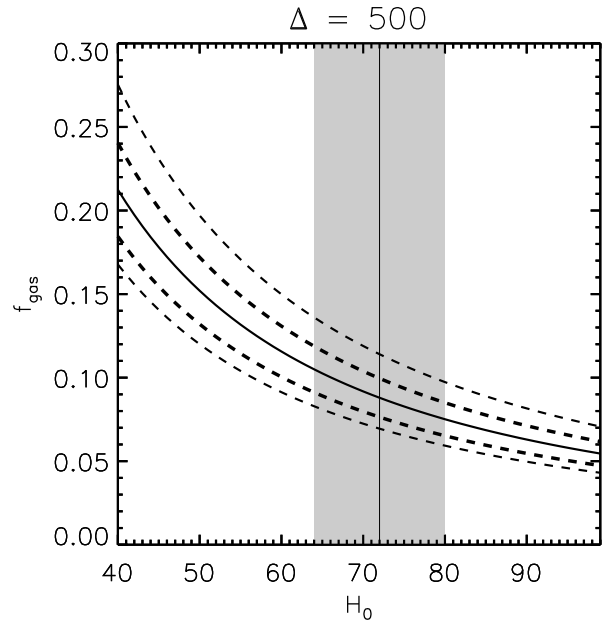


**Fig. 3.** The observed gas fraction at  $\Delta = 500$  for the eight galaxy clusters in Table 1 is here plotted as function of the Hubble constant (shaded region: constraints from Freedman et al. 2001). The solid line indicates the central value and the dashed lines the  $1$  and  $2\sigma$  uncertainties.

We plot in Fig. 3 the dependence upon the Hubble constant of the  $f_{\text{gas}}$  value ( $\propto h^{-3/2}$ ) estimated at  $\Delta = 500$  for the objects in the local sample. Assuming  $h = h_{\text{HST}} = 0.72 \pm 0.08$  (from the results of the HST Key Project on distances measured using Cepheid variables, Freedman et al. 2001) and  $\Omega_b h^2 = \Omega_{b,\text{PN}} h^2 = 0.019 \pm 0.001$  (from primeval deuterium abundance and calculations on the primordial nucleosynthesis, Burles, Nollett, Turner 2001), we obtain that  $\Omega_c$  in eqn. 5 is less than  $0.54$  (95.4 per cent confidence level).

Including a contribution from stars in galaxies of about  $f_{\text{gal}} = 0.02(\pm 0.01)h_{50}^{-1}$  (White et al. 1993, Fukugita et al. 1998) and excluding any further components to the baryon budget (see e.g. Ettori 2001), one can write  $\Omega_b/\Omega_c = f_{\text{gas}} + f_{\text{gal}} = f_b$  and, consequently from the definition of  $\Omega_m$ ,  $\Omega_b/\Omega_m = f_b/(1 + f_b)$ . (Note that the estimate of  $M_{\text{tot}}$  does not include the contribution of the gas mass, that would require the solution of a second order differential equation instead of a much simpler, and usually adopted, first order equation of the spherical hydrostatic equilibrium).

Finally, we consider the eight relaxed nearby clusters  $i$  with  $T > 4$  keV (see Table 1) to evaluate the baryon fraction at redshift  $z_i$ ,  $f_{b,i}$ , and within  $\Delta(\Omega_m = 1, \Omega_\Lambda = 0, w = -1) = 500$ . For a given set of parameters  $(\Omega_m, \Omega_\Lambda, w)$  in the range  $[0, 1]$ ,  $[0, 2]$  and  $[-1, 0]$ , respectively, we estimate  $f_{b,i}$  (and its relative error  $\epsilon_{b,i}$ ) as propagation of the estimated error on  $f_{\text{gas},i}$  and  $f_{\text{gal}}$ , where the error on  $f_{\text{gas},i}$  comes from the measured uncertainties on the gas and total mass estimates in Ettori et al. 2002, and the error on  $f_{\text{gal}}$  is  $0.01h_{50}^{-1}$ ) after considering the cosmological dependence of both  $d_{\text{ang}}$  and  $\Delta(\Omega_m, \Omega_\Lambda, w)$  (more relevant for high- $z$  systems, see Section 2) and calcu-

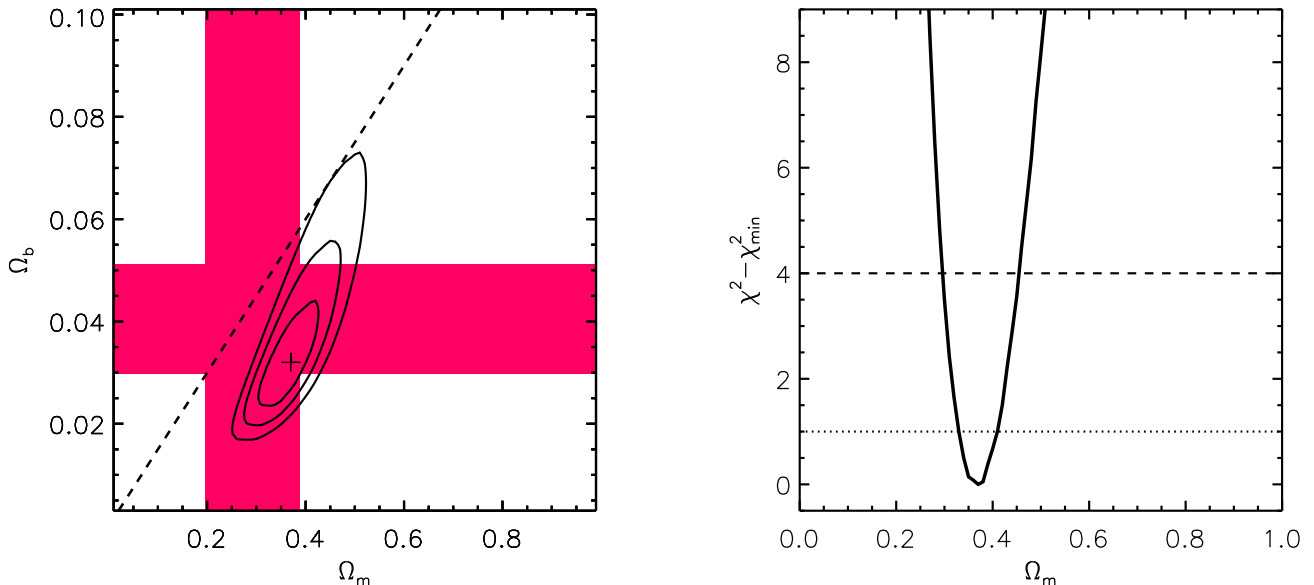


**Fig. 4.** (Left) Probability distribution contours (solid lines: 1, 2, 3 $\sigma$ ) for two interesting parameters with respect to the minimum of 29.3 in the  $\Omega_b - \Omega_m$  plane from marginalization of the likelihood provided from the baryon fraction in clusters assuming a  $f_{\text{gal}} = 0.02(\pm 0.01)h_{50}^{-1}$  (White et al. 1993; Fukugita, Hogan & Peebles 1998),  $\Omega_{b,\text{PN}}$  (Burles et al. 2001), and  $H_0 = 72 \pm 8 \text{ km s}^{-1} \text{ Mpc}^{-1}$  (Freedman et al. 2001). As reference,  $\Omega_{b,\text{CMB}}$  (horizontal shaded region) and  $\Omega_{m,\text{CMB}}$  (vertical shaded region; Netterfield et al. 2002), and  $(\Omega_b/\Omega_m)_{\text{2dF}}$  (dashed line indicates the central value; Percival et al. 2001) are indicated. (Right) Maximum likelihood distribution in the  $\Omega_m$  axis after marginalization over the other parameters (dotted line: 1 $\sigma$ , dashed line: 2 $\sigma$ ).

late

$$\chi_A^2 = \sum_i \frac{(f_{b,i} - \Omega_b/\Omega_m)^2}{\epsilon_{b,i}^2} + \frac{(\Omega_b - \Omega_{b,\text{PN}})^2}{\epsilon_{\Omega_b}^2} + \frac{(h - h_{\text{HST}})^2}{\epsilon_h^2}, \quad (6)$$

where  $\Omega_{b,\text{PN}}$  and  $h_{\text{HST}}$  are defined above.

The  $\chi^2$ -distribution in eqn. 6 is used to construct a  $\Delta\chi^2$  statistics,  $\Delta\chi^2 = \chi_A^2 - \chi_{A,\text{min}}^2$ , by which we generate regions and intervals of confidence (e.g., the 1 $\sigma$  level of confidence for one and two degrees of freedom is  $\Delta\chi^2 = 1$  and 2.3, respectively).

Marginalizing over the accepted ranges of Hubble constant from the HST Key Project (Freedman et al. 2001) and  $\Omega_b$  from primordial nucleosynthesis, we obtain (2 $\sigma$ )  $\Omega_m = 0.37^{+0.07}_{-0.08}$  and  $\Omega_b = 0.032^{+0.017}_{-0.010}$ , that are well in agreement with  $\Omega_{m,\text{CMB}}$  from CMB and  $\Omega_b/\Omega_m$  from large scale structures analysis of the “2dF” data (see Figure 4).

#### 4. SECOND CONSTRAINT: GAS FRACTION CONSTANT IN TIME

In this section, we present a sample of galaxy clusters with  $z > 0.7$  and compute their gas mass fraction. These values are compared to the local estimates to put cosmological constraints under the assumption that the gas fraction remains constant with redshift when computed at the same density contrast.

It is worth noticing that this method, originally proposed from Sasaki (1996; see also Cooray 1998, Danos & Ue-Li Pen 1998, Rines et al. 1999, Ettori & Fabian 1999b, Allen et al. 2002), does not require any *prior* on the values of  $\Omega_b$  and  $H_0$ , taking into account just the relative variation of the gas fraction as function of time. In other words, the method assumes that gas fraction in galaxy clusters can be used like a “standard candle” to measure the geometry of the Universe. This is a reasonable assumption in any hierarchical clustering scenario when the energy of the ICM is dominated by the gravitational heating and is supported by numerical and semianalytical models for the thermodynamics of the ICM, also when including preheating and cooling effects. In recent hydrodynamical simulations with an entropy level of 50 keV cm $^{-2}$  generated in the cluster at  $z = 3$  (see Borgani et al. 2002), the baryon fraction in clusters with an observed temperature around 3 keV is constant in time within few percent (see also figure 13 in Bialek, Evrard and Mohr 2001). Similar results are obtained in the semianalytical model of Tozzi & Norman (2001), where a constant entropy floor is initially present in the cosmic baryons. In Figure 5, we show the prediction for the baryonic fraction (in terms of the universal value) within an average overdensity  $\Delta = 1500$  as a function of the emission weighted temperature  $T_{ew}$ , computed in a  $\Lambda$ CDM cosmology and with an entropy level of  $0.3 \times 10^{34}$  erg cm $^2$  g $^{-5/3}$  (see Tozzi & Norman 2001 for details). A significant decrease of the baryonic fraction is expected at  $z = 1$  (dashed line) with respect to the local value (solid line) only for

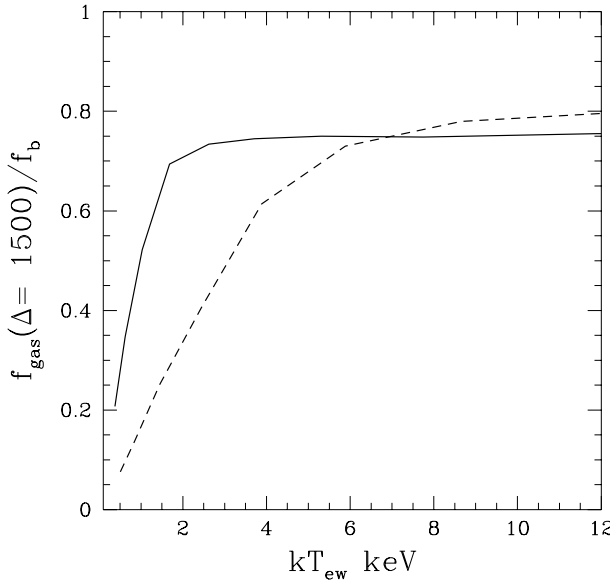


**Fig. 5.** The gas fraction in unit of the cosmic baryon budget at  $\Delta = 1500$  as a function of the observed (emission weighted) temperature computed for the model of Tozzi & Norman (2001) with a constant entropy of  $0.3 \times 10^{34}$  erg cm $^2$  g $^{-5/3}$  in a  $\Lambda$ CDM ( $\Omega_m = 1 - \Omega_\Lambda = 0.3$ ) Universe. The *solid line* is for  $z = 0$ , and the *dashed line* for  $z = 1$ . Note the 20 per cent offset from the universal value, which reduces to 10 per cent for  $\Delta = 500$  (see comments on the baryonic depletion in Section 5).

temperatures below 4 keV. In particular, at temperatures above 6 keV, the baryonic fraction is constant or possibly 5 per cent higher at  $z = 1$  with respect to  $z = 0$ . This strongly supports the assumption of a baryon fraction constant with the cosmic epoch for clusters with  $kT > 4$  keV.

With this assumption, we expect to measure a constant average gas fraction locally and in distant clusters. However, the gas fraction is given by a combination of the observed flux and of the angular distance, and thus it depends on cosmology (see discussion in Section 2). As shown in Figure 1, the high redshift objects are more affected from this dependence and show lower  $f_{\text{gas}}$  with respect to the local values when universes with high matter density are assumed. By requiring the measured gas fractions to be constant as a function of redshift, one can constrain the range of values of cosmological parameters which satisfies such a condition.

#### 4.1. The high- $z$ sample

We define a local sample considering all the relaxed systems in Ettori et al. (2002) that have a mass-weighted temperature larger than 4 keV within  $\Delta = 1500$  (cf. Table 1). Within this density contrast, we measure  $f_{\text{gas}}$  as described in Section 2. The density contrast is chosen to be 1500 as a good compromise between the cluster regions directly observed in the

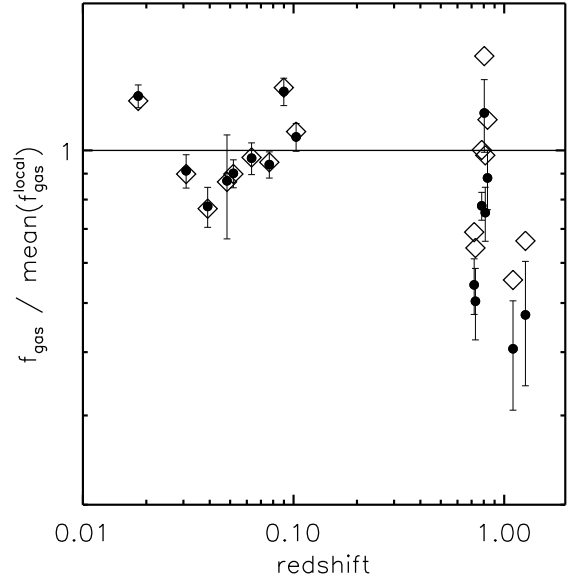


**Fig. 6.** Distribution as function of redshift of the gas fraction relative to the mean local value and estimated for the clusters in our sample at the same overdensity  $\Delta = 1500$ . *Filled circles* are the values calculated in an Einstein-de Sitter universe, whereas *diamonds* indicate the results for a low density universe ( $\Omega_m = 1 - \Omega_\Lambda = 0.3$ ).

nearby systems and those with relevant X-ray emission in the high- $z$  objects. This sample includes eight high redshift ( $z > 0.7$ ) hot ( $T > 4$  keV) clusters, six of which selected from the *ROSAT* Deep Cluster Survey (Rosati et al. 1998) and recently observed with *Chandra* (Stanford et al. 2001, Holden et al. 2002). We reprocess the level=1 events files retrieved from the archive and obtain a spectrum and an image for each cluster (see details in Tozzi et al., in preparation). Seven of these objects were observed in ACIS-I mode (only MS1054 has been observed with the back-illuminated S3 CCD). Following the prescription in Markevitch & Vikhlinin (2001), the effective area below 1.8 keV in the front-illuminated CCD is corrected by a factor 0.93 to improve the cross calibration with back-illuminated CCDs. The spectrum extracted up to the radius  $r_{\text{out}}$  to optimize the signal-to-noise ratio is modelled between 0.8 and 7 keV with an absorbed optically-thin plasma (wabs (mekal) in XSPEC v. 11.1.0, Arnaud 1996) with fixed redshift, galactic absorption (from radio HI maps in Dickey & Lockman 1990) and metallicity (0.3 times the solar values in Anders & Grevesse 1989) and using a local background obtained from regions of the same CCD free of any point source. The gas temperature and the normalization  $K$  of the thermal component are the only free parameters. The surface brightness profile obtained from the image is fitted with an isothermal  $\beta$ -model (Cavaliere & Fusco-Femiano 1976, Ettori 2000), which provides an analytic expression for the gas density and total mass of the cluster. In particular, the central electron density is obtained from the combination of the best-fit results from

**Table 2.** The high redshift sample from Chandra observations. The results are obtained applying a  $\beta$ -model in an Einstein-de Sitter universe with a Hubble constant of  $50 \text{ km s}^{-1} \text{ Mpc}^{-1}$ . All the quoted errors are at  $1\sigma$  level. Note that MS1054.5-0321 presents significant substructure (e.g. Jeltema et al. 2001). The temperature and the best-fit of the surface brightness profile are estimated from the main body of the cluster once a circular region centered at (RA, Dec; 2000)=( $10^{\text{h}}56^{\text{m}}55^{\text{s}}7, -3^{\circ}37'37''$ ) and with radius of 36 arcsec is masked.

cluster	$z$	$r_{\text{out}}$ "/ kpc	$T_{\text{gas}}$ keV	$r_c$ kpc	$\beta$	$n_{\text{ele}}(0)$ $10^{-2} \text{ cm}^{-3}$	$M_{\text{tot}}(r_{\text{out}})$ $10^{13} M_{\odot}$	$\Delta(r_{\text{out}})$	$f_{\text{gas}}(r_{\text{out}})$
RDCS J0849+4452	1.261	29.5 / 254	$5.0^{+1.4}_{-1.0}$	$104^{+52}_{-31}$	$0.70^{+0.27}_{-0.14}$	$0.93^{+0.20}_{-0.17}$	$8.6^{+2.7}_{-2.4}$	$1559^{+490}_{-427}$	$0.055^{+0.018}_{-0.014}$
RDCS J0910+5422	1.101	29.5 / 253	$5.0^{+1.3}_{-1.0}$	$110^{+68}_{-40}$	$0.64^{+0.34}_{-0.16}$	$0.82^{+0.19}_{-0.14}$	$7.7^{+2.5}_{-1.8}$	$1748^{+580}_{-405}$	$0.053^{+0.014}_{-0.013}$
MS1054.5-0321	0.833	82.7 / 685	$10.1^{+1.1}_{-0.9}$	$576^{+46}_{-49}$	$1.36^{+0.15}_{-0.14}$	$0.54^{+0.01}_{-0.01}$	$61.2^{+7.2}_{-5.7}$	$1062^{+124}_{-98}$	$0.106^{+0.011}_{-0.011}$
RDCS J1716.9+6708	0.813	33.5 / 276	$7.1^{+1.0}_{-0.8}$	$116^{+14}_{-13}$	$0.60^{+0.03}_{-0.03}$	$1.35^{+0.14}_{-0.11}$	$11.2^{+1.5}_{-1.3}$	$3061^{+413}_{-354}$	$0.079^{+0.012}_{-0.011}$
RDCS J1350.0+6007	0.804	68.9 / 567	$4.1^{+0.8}_{-0.6}$	$194^{+54}_{-40}$	$0.57^{+0.12}_{-0.07}$	$0.46^{+0.06}_{-0.05}$	$13.5^{+3.0}_{-2.7}$	$433^{+97}_{-85}$	$0.170^{+0.040}_{-0.030}$
MS1137.5+6625	0.782	45.3 / 370	$6.3^{+0.4}_{-0.4}$	$115^{+7}_{-7}$	$0.67^{+0.02}_{-0.02}$	$1.69^{+0.07}_{-0.07}$	$15.8^{+1.2}_{-1.0}$	$1890^{+144}_{-131}$	$0.114^{+0.008}_{-0.008}$
WARPS J1113.1-2615	0.730	51.2 / 412	$5.0^{+0.8}_{-0.7}$	$110^{+25}_{-22}$	$0.66^{+0.12}_{-0.09}$	$0.97^{+0.11}_{-0.10}$	$14.3^{+2.6}_{-2.5}$	$1355^{+251}_{-239}$	$0.071^{+0.014}_{-0.011}$
RDCS J2302.8+0844	0.720	49.2 / 394	$6.7^{+1.1}_{-0.9}$	$118^{+20}_{-17}$	$0.57^{+0.06}_{-0.05}$	$0.74^{+0.06}_{-0.05}$	$15.4^{+2.4}_{-2.3}$	$1688^{+261}_{-257}$	$0.068^{+0.012}_{-0.011}$

the spectral and imaging analyses as follows:

$$n_{0,\text{ele}}^2 = \frac{4\pi d_{\text{ang}}^2 \times (1+z)^2 \times K \times 10^{14}}{0.82 \times 4\pi r_c^3 \int_0^{r_{\text{out}}} (1+x^2)^{-3\beta} x^2 dx} \quad (7)$$

where  $(\beta, r_c)$  are the best-fit parameters of the  $\beta$ -model and we assume  $n_p = 0.82 n_e$  in the ionized intra-cluster plasma. After 1000 random selections of a temperature, normalization and surface brightness profile (drawn from Gaussian distributions with mean and variance in accordance to the best-fit results), we obtain a distribution of the estimates of the gas and total mass and of the gas mass fraction. We adopt for each cluster the median value and the 16th and 84th percentile as central and  $1\sigma$  value, respectively (see Table 2).

In Figure 6, we plot  $f_{\text{gas}}$  of the clusters in exam as a function of redshift, as computed in an Einstein-de Sitter (filled dots) and a low density ( $\Omega_m = 1 - \Omega_\Lambda = 0.3$ ) universe (open squares).

#### 4.2. The analysis

We compare our local estimate of the gas mass fraction with the values observed in the objects at  $z > 0.7$  within the same density contrast  $\Delta = M_{\text{tot}}(< r_\Delta) / (4\pi \rho_{c,z} r_\Delta^3)$ , where  $M_{\text{tot}}(< r_\Delta)$  is estimated from the  $\beta$ -model. Initially, we estimate the gas fraction for all the clusters at  $\Delta = 1500$  in an Einstein-de Sitter universe. Then, we proceed as described in Section 2.

As discussed above, we consider a set of parameters  $(\Omega_m, \Omega_\Lambda)$  in the range  $[0, 1]$  and  $[0, 2]$ , respectively, both fixing  $w$  equals to  $-1$  as prescribed for the “cosmological constant” case and exploring the range  $w \in [-1, 0]$  (in this case, we require  $\Omega_k = 0$ ), and evaluate the distribution

$$\chi_B^2 = \sum_j \frac{[f_{\text{gas},j}(\Omega_m, \Omega_\Lambda) - \bar{f}_{\text{gas}}]^2}{\epsilon_{\text{gas},j}^2 + \bar{\epsilon}_{\text{gas}}^2}, \quad (8)$$

where  $\bar{f}_{\text{gas}}$  and  $\bar{\epsilon}_{\text{gas}}$  are the mean and the standard deviation of the values of the gas fraction in the *local* cluster sample, and  $\epsilon_{\text{gas},j}$  is the error on the measurement of  $f_{\text{gas},j}$  for  $j \in [\text{high-}z \text{ sample}]$ . It is worth noticing that the use of the standard deviation around the mean is a conservative approach. For example, at  $(\Delta, \Omega_m, H_0) = (1500, 1, 50)$ , we measure a mean of

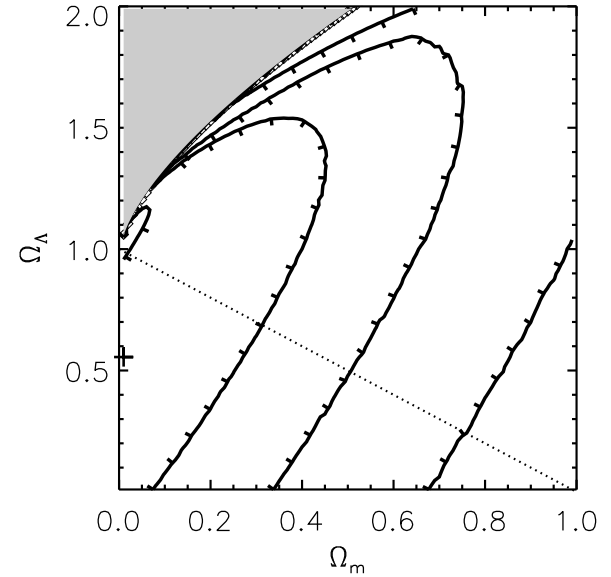


**Fig. 7.** Maximum likelihood distributions in the “ $\Omega_m + \Omega_\Lambda + \Omega_k = 1$ ” region obtained from the application of the method that requires “ $f_{\text{gas}} = \text{constant}$ ” (cf. Section 4; shaded region: no-big-bang solution, dotted line: “ $\Omega_k = 0$ ” region). The contours enclose the regions with  $\Delta\chi^2 = 2.30, 6.17, 11.8$  (with respect to the minimum of 11.7 with eight objects in exam), corresponding to 1, 2, 3  $\sigma$ , respectively, for a distribution with two interesting parameters.

0.134 and standard deviation of 0.025, the latter being about 8 times larger than the measured error on the weighted mean and slightly larger than the dispersion obtained with the Bayesian method illustrated in Fig. 2. Using just the results obtained on the  $\chi_B^2$  distribution, we obtain a best-fit solution that requires the following upper limits at  $2\sigma$  level (one interesting parameter),  $\Omega_m < 0.60$  and  $\Omega_\Lambda < 1.69$  (cf. Figure 7).

## 5. SYSTEMATIC UNCERTAINTIES

The intrinsic scatter in the distribution of the  $f_{\text{gas}}$  values of approximately 20 per cent is the most relevant statistical uncertainty affecting our cosmological constraints. We discuss in this section how a number of systematic uncertainties contribute to a lesser extent.

– We have assumed that the intracluster medium is in hydrostatic equilibrium, distributed with a spherical geometry, with no significant (i) clumpiness in the X-ray emitting plasma, (ii) depletion of the cosmic baryon budget at the reference radius, and (iii) contribution from non-thermal components. The hydrostatic equilibrium in a spherical potential is widely verified to be a correct assumption for local clusters, but it cannot be the case (in particular on the geometry of the plasma distribution, but see Buote & Canizares 1996) for high redshift clusters. The level of clumpiness in the plasma expected from numerical simulations (e.g. Mohr et al. 1999) induce an overestimate of the gas fraction. On the other hand, the expected baryonic depletion (still from simulations; e.g. Frenk et al. 1999) underestimates the observed cluster baryon budget by an amount that can be comparable (but of opposite sign) to the effect of the clumpiness (see discussion in Ettori 2001). For the high redshift objects observed within  $\Delta=1500$ , a larger clumpiness can be present as consequence of on-going process of formation that, on the other hand, might still partially compensate for a residual depletions of baryons observed in the simulations in the range 4–6 keV (cfr. Figure 5). The combination of these effects induce however an uncertainty in the relative amount of baryons of less than 10 per cent, percentage that is below the observed statistical uncertainties.

Moreover, the radial dependence of  $f_{\text{gas}}$  can be slightly steeper in the inner cluster regions due to the relative broader distribution of the gas with respect to the dark matter (but see Allen et al. 2002 for  $f_{\text{gas}}$  profiles observed flat within  $\Delta=2500$ ). Finally, from the remarkable match between the gravitational mass profiles obtained independently from X-ray and lensing analysis (e.g. Allen, Schmidt & Fabian 2001), it seems negligible any non-thermal contribution to the total mass apart from a possible role played in the inner regions.

– The high redshift sample has been analyzed using an isothermal  $\beta$ –model. From recent analyses of nearby clusters with spatially resolved temperature profiles, it appears that this method can still provide a reasonable constraint on the gas density, but surely affect the estimate of the total mass, in particular in the outskirts and, more dramatically, when an extrapolation is performed. On the other hand, the physical properties of nearby clusters at overdensity of 1500 (e.g. Ettori et al. 2002) guarantee that the expected gradient in temperature is not significantly steep and, therefore, does not affect the estimate of the total gravitating mass. However, the presence of a gradient in the temperature profile would reduce the total mass measurements and increase, consequently, the derived gas mass fraction.

– We assume that relaxed nearby and high- $z$  clusters, both with  $T_{\text{gas}} > 4$  keV, represent a homogeneous class of ob-

jects. If we relax this assumption and include non-relaxed nearby systems (or equivalently no-cooling-flow clusters in the sample of Ettori et al. 2002), we obtain the same cosmological constraints though the scatter in the distribution of the gas fraction values becomes larger (e.g., at  $\Delta=1500$ , the scatter is 0.025 for relaxed systems only and 0.033 for the complete sample).

In conclusion, we check our results against two effects: (i) by increasing the gas mass fraction in the high- $z$  sample by a factor 1.15, and (ii) by changing the slope of the radial dependence of  $f_{\text{gas}}(r)$  (cfr. factor  $F_2$  in Section 2) by  $\pm 0.1$ . All these corrections do not change significantly the results quoted in the next section on  $\Omega_m$  due to heavier statistical weight given from the first method, that is the one less (or completely not) affected from the above mentioned effects. On the other hand, they mostly affect the second method in such a way that (i) gas fraction values at high- $z$  higher by 15 per cent reduce the  $2\sigma$  upper limit on  $\Omega_\Lambda$  by 10 per cent, but increase the one on  $w$  by 50 per cent, (ii) steeper radial  $f_{\text{gas}}$  profiles (i.e. larger dependence upon the density contrast  $\Delta$ ) raise the limit on  $\Omega_\Lambda$ , but have not relevant effects on  $w$ . In details, when the slope changes from 0 to  $-0.1$  and  $-0.2$ , the upper limit on  $\Omega_\Lambda$  increases from 25 to 5 per cent, respectively.

## 6. CONCLUSIONS

We show how the combined likelihood analysis of (i) the representative value of  $f_{\text{gas}}$  in clusters of galaxies and (ii) the requirement that  $f_{\text{gas}}(z) = \text{constant}$  for an assumed homogeneous class of objects with  $T > 4$  keV can set stringent limits on the dark matter density and any further contribution to the cosmic energy, i.e.  $\Omega_m$  and  $\Omega_\Lambda$  respectively.

First, a total  $\chi^2$  distribution is obtained by combining the two distributions presented in eqn. 6 and 8, i.e.  $\chi^2 = \chi_A^2 + \chi_B^2$ . The resulting likelihood contours (Figure 8) are obtained marginalizing over the range of parameters not investigated. With further *a priori* assumptions on  $\Omega_b$  and  $H_0$ , and assuming a flat geometry of the universe, we constrain (see right panel in Figure 8) the dark energy pressure-to-density ratio to be

$$w < -0.85(1\sigma), -0.54(2\sigma), -0.23(3\sigma). \quad (9)$$

This constraint is in excellent agreement with the bound on  $w$  obtained with independent cosmological datasets, such as the angular power spectra of the Cosmic Microwave Background, the magnitude-redshift relation probed by distant type Ia Supernovae and the power spectrum obtained from the galaxy distribution in the two-degrees-field (for a combined analysis of these datasets, see, e.g., Hannestad & Mörtsell 2002 and reference therein). Moreover, this upper bound is completely in agreement with  $w = -1$  as required for the equation of state of the “cosmological constant”. Fixing  $w = -1$ , we obtain (for one interesting parameter)

$$\begin{aligned} \Omega_m &= 0.34^{+0.07}_{-0.03}(1\sigma), & +0.11^{+0.11}_{-0.05}(2\sigma), & +0.16^{+0.16}_{-0.08}(3\sigma) \\ \Omega_\Lambda &= 1.50^{+0.20}_{-0.55}(1\sigma), & +0.24^{+0.24}_{-1.13}(2\sigma), & +0.30^{+0.30}_{-0.08}(3\sigma). \end{aligned} \quad (10)$$

Finally, imposing a flat Universe (i.e.  $\Omega_k = 0$ ) as the recent constraints from the angular power spectrum of the cosmic microwave background indicate (e.g. de Bernardis et al. 2002 and

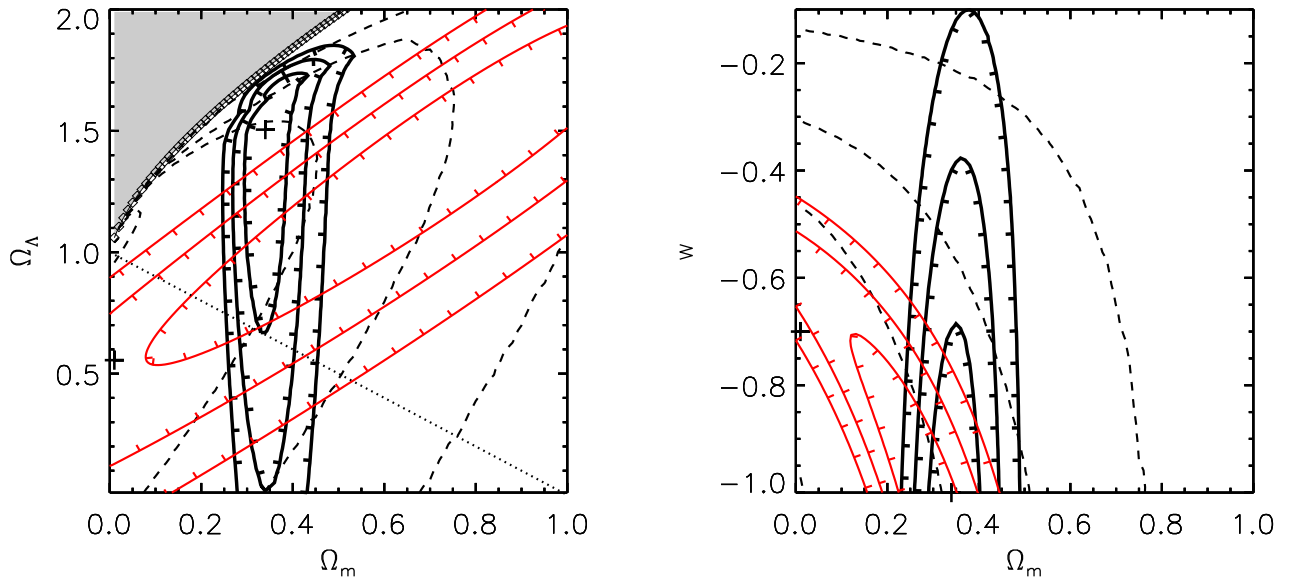


**Fig. 8.** (Left) Maximum likelihood distributions in the “ $\Omega_m + \Omega_\Lambda + \Omega_k = 1$ ” region. Contour plots (thick solid lines) from the combination of the two likelihood distributions ( $A$ : cluster baryonic content,  $B$ : gas fraction constant with redshift; dashed lines indicate the constraints from the second method only, see Fig. 7; the cross indicates the best-fit result at  $\Omega_m = 0.34$ ,  $\Omega_\Lambda = 1.18$ ) with overplotted the constraints from the magnitude-redshift method applied to a set of SN Ia (cf. Leibundgut 2001, thin solid lines). (Right) Constraints on the parameter  $w$  of the cosmological equation of state (thick solid lines from the combination of the method  $A$  and  $B$ ; dashed lines from the second method only; the crosses show the best-fit results, that is located at  $\Omega_m = 0.35$  and  $w = -1$  for the combined probability distribution). The thin solid lines indicate the constraints from SN Ia (P. Garnavich, priv. comm.; updated version of Garnavich et al. 1998 combining Riess et al. 1998 and Perlmutter et al. 1999 data sets). The contours enclose the regions with  $\Delta\chi^2 = 2.30, 6.17, 11.8$ , corresponding to 1, 2, 3  $\sigma$ , respectively, for a distribution with two degrees-of-freedom.

references therein), we obtain that  $\Omega_m = 1 - \Omega_\Lambda = 0.33^{+0.06}_{-0.05}$  at 95.4 per cent confidence level.

Our limits on cosmological parameters fit nicely in the cosmic concordance scenario (Bahcall et al. 1999, Wang et al. 2000), with a remarkable good agreement with independent estimates derived from the angular power spectrum of Cosmic Microwave Background (Netterfield et al. 2002, Sievers et al. 2002), the magnitude–redshift relation for distant supernovae type Ia (Riess et al. 1998, Perlmutter et al. 1999; the likelihood region from a sample of SN type Ia as described in Leibundgut 2001 is shown in Figure 8, panel at the bottom-left), the power spectrum from the galaxy distribution in the 2dF Galaxy Redshift Survey (e.g., Efstathiou et al. 2002) and from galaxy clusters (e.g. Schuecker et al. 2002), the evolution of the X-ray properties of clusters of galaxies (e.g. Borgani et al. 2001, Arnaud, Aghanim & Neumann 2002, Henry 2002, Rosati, Borgani & Norman 2002). For example, combining the constraints in Figure 8 between the allowed regions from the gas mass fraction and the magnitude–redshift relation for SN-Ia, we obtain (2  $\sigma$  statistical error)  $\Omega_m = 0.34^{+0.07}_{-0.05}$  and  $\Omega_\Lambda = 0.94^{+0.30}_{-0.30}$ . These values are 0.5 and 0.6  $\sigma$  higher, respectively, than the CMB constraints obtained with the SN-Ia prior (see Table 4 in Netterfield et al. 2002). Moreover, by combining  $f_{\text{gas}}$  and SN-Ia measurements we can obtain a very

tight constraint on  $w$  (right panel in Figure 8):  $w < -0.89$  and  $\Omega_m = 0.32^{+0.05}_{-0.05}$  at the 95.4 per cent confidence level.

We have demonstrated how the measurements of the cluster gas mass fraction represent a powerful tool to constrain the cosmological parameters and, in particular, the cosmic matter density,  $\Omega_m$ . Nonetheless, the limits on  $\Omega_\Lambda$  and  $w$ , though weaker, provide a complementary and independent estimate with respect to the most recent experiments in this field. On this item, it is worth noticing that our constraints on  $\Omega_\Lambda$  are mostly due to the  $d_{\text{ang}}$  dependence of  $f_{\text{gas}}$  (cf. Fig. 1). Thus, a larger sample of high- $z$  clusters with accurate measurements of the gas mass fraction will significantly shrink the confidence contours, as we show in Figure 9. Compilations of such datasets will be possible in the near future using moderate-to-large area surveys obtained from observations with *Chandra* and *XMM-Newton* satellites.

## ACKNOWLEDGEMENTS

We thank Stefano Borgani and Peter Schuecker for very useful discussions. Bruno Leibundgut and Peter Garnavich are thanked for proving us the likelihood distributions from supernovae type Ia plotted in Figure 8. Pat Henry gave us a list of formula in advance of publication that was useful to check our definition of the density contrast. The anonymous referee is

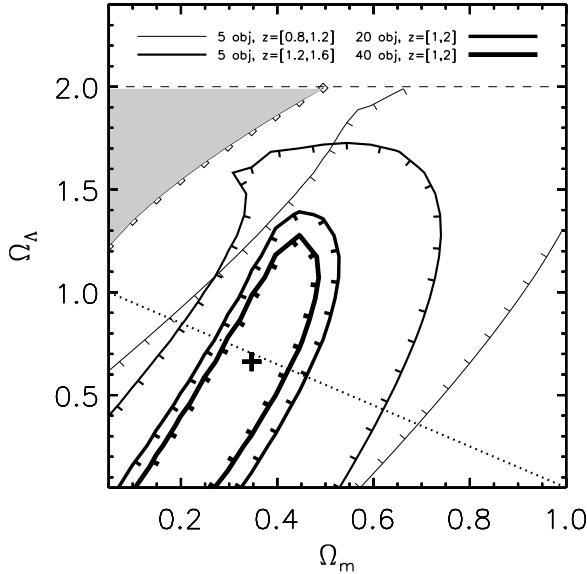


**Fig. 9.** Constraints in the  $\Omega_m - \Omega_\Lambda$  plane as in Fig. 7 for simulated sets of gas mass fraction measurements. The contours are at  $1\sigma$  confidence level. A cosmological model with  $\Omega_m = 1 - \Omega_\Lambda = 0.34$  is assumed and only the  $d_{\text{ang}}^{3/2}$  dependence is considered. In the redshift range [1, 2], the increase by a factor of two of the sample allows to reduce the upper limit on  $\Omega_\Lambda$  by about 10 per cent.

thanked for useful comments. PT acknowledges support under the ESO visitor program in Garching.

## References

Allen S.W., Schmidt R.W., Fabian A.C., 2001, MNRAS, 328, L37  
 Allen S.W., Schmidt R.W., Fabian A.C., 2002, MNRAS, 334, L11  
 Anders E., Grevesse N., 1989, Geochimica et Cosmochimica Acta, 53, 197  
 Arnaud K.A., 1996, "Astronomical Data Analysis Software and Systems V", eds. Jacoby G. and Barnes J., ASP Conf. Series vol. 101, 17  
 Arnaud M., Aghanim N., Neumann D.M., 2002, A&A, 389, 1  
 Bahcall N.A., Ostriker J.P., Perlmutter S., Steinhardt P.J., 1999, Sci, 284, 1481  
 de Bernardis et al., 2002, ApJ, 564, 559  
 Bialek J.J., Evrard A.E., Mohr J.J. 2001, ApJ, 555, 597  
 Borgani S., Rosati P., Tozzi P., et al., 2001, ApJ, 561, 13  
 Borgani S., Governato F., Wadsley J., Menci N., Tozzi P., Quinn T., Stadel J., Lake G., 2002, MNRAS, 336, 409  
 Buote D.A., Canizares C.R., 1996, ApJ, 457, 565  
 Burles S., Nollett K.M., Turner M.S., 2001, ApJ, 552, L1  
 Caldwell R.R., Dave R., Steinhardt P.J., 1998, Phys. Rev. Lett., 80, 1582  
 Cavaliere A., Fusco-Femiano R., 1976, A&A, 49, 137  
 Carroll S.M., Press W.H., Turner E.L., 1992, ARAA 30, 499  
 Cooray A.R., 1998, A&A 333, L71  
 Danos R., Ue-Li Pen, 1998, astro-ph/9803058  
 David L.P., Jones C., Forman W., 1995, ApJ, 445, 578  
 Dickey J.M., Lockman, F.J., 1990, ARA&A, 28, 215  
 Efstathiou G., Bridle S.L., Lasenby A.N., Hobson M.P., Ellis R.S., 1999, MNRAS 303, 47  
 Efstathiou G. et al., 2002, MNRAS, 330, L29  
 Elgaroy O. et al., 2002, Phys. Rev. Lett., in press (astro-ph/0204152)  
 Erdogdu P., Ettori S., Lahav O., 2002, MNRAS, submitted (astro-ph/0202357)  
 Ettori S., Fabian A.C., 1999a, MNRAS 305, 834  
 Ettori S., Fabian A.C., 1999b, proceedings of the Ringberg workshop on "Diffuse Thermal and Relativistic Plasma in Galaxy Clusters", H. Böhringer, L. Feretti, P. Schuecker (eds.), MPE Report No. 271, MPE Garching  
 Ettori S., 2000, MNRAS, 311, 313  
 Ettori S., 2001, MNRAS, 323, L1  
 Ettori S., De Grandi S., Molendi S., 2002, A&A, 391, 841  
 Evrard A.E., 1997, MNRAS 292, 289  
 Freedman W. et al., 2001, ApJ, 553, 47  
 Frenk C.S. et al., 1999, ApJ, 525, 554  
 Fukugita M., Hogan C.J., Peebles P.J.E., 1998, ApJ, 503, 518  
 Garnavich P. et al., 1998, ApJ, 509, 74  
 Gerke B.F., Efstathiou G., 2002, MNRAS, 335, 33  
 Hannestad S., Mörtsell E., 2002, astro-ph/0205096  
 Hannestad S., 2002, astro-ph/0205223  
 Henry J.P., 2002, "Matter and Energy in Clusters of Galaxies", eds. Hwang Y. and Bowyer S., ASP Conf. Series, in press (astro-ph/0207148)  
 Holden B.P., Stanford S.A., Squires G.K., Rosati P., Tozzi P., Eisenhardt P., Spinrad H., 2002, AJ, 124, 33  
 Huterer D., Turner M.S., 2001, Phys. Rev. D, 64, 123527  
 Jeltema T.E., Canizares C.C., Bautz M.W., Malm M.R., Donahue M., Garmire G.P., 2001, ApJ, 562, 124  
 King I.R., 1962, AJ, 67, 471  
 Leibundgut B., 2001, ARAA, 39, 67  
 Lokas E., Hoffman Y., 2001, MNRAS, submitted (astro-ph/0108283)  
 Markevitch M., Vikhlinin A., 2001, ApJ, 563, 95  
 Mohr J.J., Mathiesen B., Evrard A.E., 1999, ApJ, 517, 627  
 Navarro J.F., Frenk C.S., White S.D.M., 1997, ApJ, 490, 493  
 Netterfield C.B. et al., 2002, ApJ, 571, 604  
 Peebles P.J.E., Ratra B., 2002, astro-ph/0207347  
 Percival W.J. et al., 2001, MNRAS, submitted (astro-ph/0105252)  
 Perlmutter S. et al., 1999, ApJ, 517, 565  
 Ponman T.J., Cannon, D.B., Navarro, J.F. 1999, Nature, 397, 135  
 Press W.H., 1996, in "Unsolved Problems in Astrophysics", Proceedings of Conference in Honor of John Bahcall, J.P. Ostriker ed., Princeton University Press (astro-ph/9604126)  
 Riess A.G. et al., 1998, AJ, 116, 1009  
 Rines K., Forman W., Pen U., Jones C., Burg R., 1999, ApJ 517, 70  
 Rosati P., della Ceca R., Norman C., Giacconi R., 1998, ApJ, 492, L21  
 Rosati P., Borgani S., Norman C., 2002, ARAA, 40, in press  
 Roussel H., Sadat R., Blanchard A., 2000, A&A, 361, 429  
 Sasaki S., 1996, PASJ 48, L119  
 Schuecker P., Böhringer H., Collins C.A., Guzzo L., 2002, A&A, submitted (astro-ph/0208251)  
 Sievers J.L. et al., 2002, ApJ, submitted (astro-ph/0205387)  
 Stanford S.A., Holden B.P., Rosati P., Tozzi P., Borgani S., Eisenhardt P., Spinrad H., 2001, ApJ, 552, 504  
 Tozzi, P., & Norman, C. 2001, ApJ, 546, 63  
 Turner M.S., White M., 1997, Phys. Rev. D, 56 (8), 4439  
 Wang L., Steinhardt P.J., 1998, ApJ, 508, 483  
 Wang L., Caldwell R.R., Ostriker J.P., Steinhardt P.J., 2000, ApJ, 530, 17  
 White D.A., Fabian A.C., 1995, MNRAS, 273, 72  
 White S.D.M., Navarro J.F., Evrard A.E., Frenk C.S., 1993, Nature 366, 429

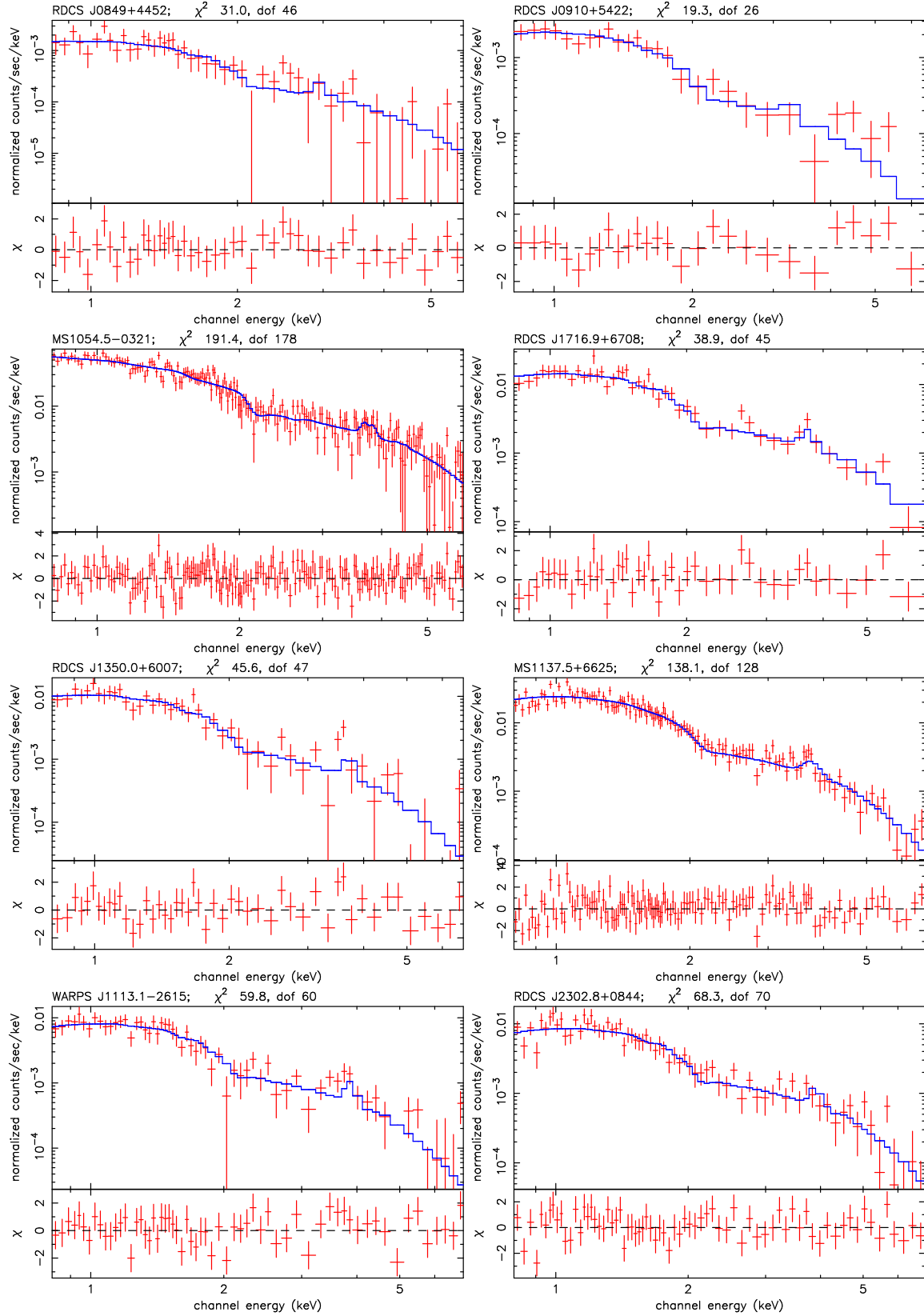


**Fig. A-1.** Data and best-fit MEKAL model of the spectrum of the galaxy clusters at high redshift in our sample.

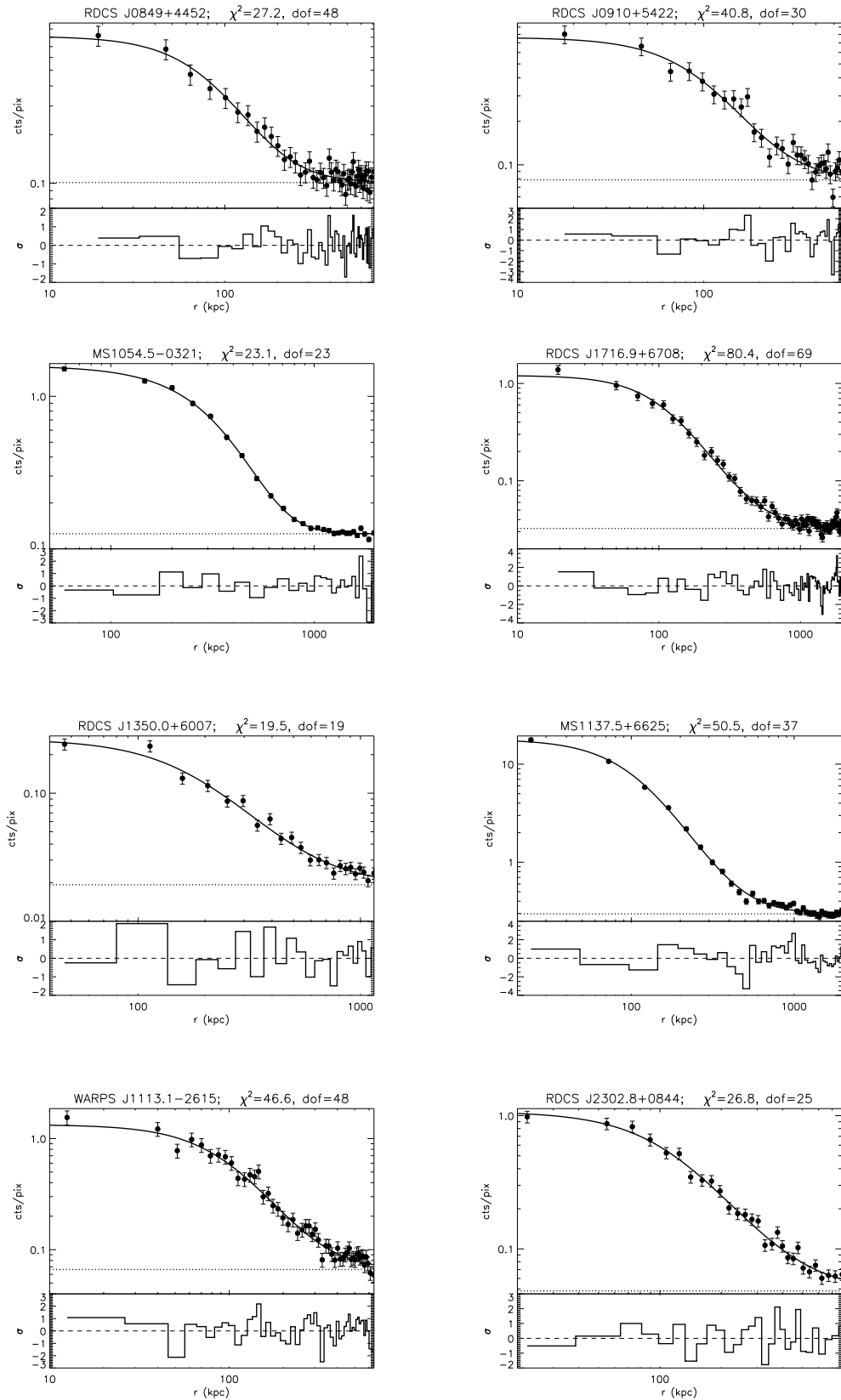


**Fig. A-2.** Data and best-fit  $\beta$ -model of the surface brightness profile of the galaxy clusters at high redshift in our sample. Dotted lines indicate the best-fit background value.